Influence of volcanic glass on the magnetic signal of different paleosols in Córdoba, Argentina

SABRINA ROUZAUT[1,2] AND MARÍA JULIA ORGEIRA[3,4]

1 Centro de Investigaciones en Ciencias de la Tierra (CICTERRA). Consejo Nacional de Investigaciones Científicas y Técnicas (CONICET) y Universidad Nacional de Córdoba. Av. Vélez Sarsfield 1611, X5016CGA, Córdoba, Argentina

2 Facultad de Ciencias Exactas, Físicas y Naturales, Universidad Nacional de Córdoba. Av. Vélez Sarsfield 1611, X5016CGA, Córdoba, Argentina (srouzaut@unc.edu.ar)

3 IGEBA, Consejo Nacional de Investigaciones Científicas y Técnicas (CONICET) y Universidad Nacional de Buenos Aires. Ciudad Universitaria Pab. II, Nuñez, Buenos Aires, Argentina

4 Dpto. Ciencias Geológicas, Facultad de Ciencias Exactas y Naturales, Universidad de Buenos Aires, Buenos Aires, Argentina

Received: June 27, 2016; Revised: August 18, 2016; Accepted: October 4, 2016

ABSTRACT

This contribution comprises geological and magnetic results obtained in loess and paleosols profiles outcropped in the Pampean plain (Argentina). The sedimentary sequence exposed in Córdoba province is represented by four profiles Corralito I, Corralito II, Monte Ral815o and Lozada, 32°S 64°14'W (Argentina). These profiles were mineralogically described and magnetically analyzed. The sediments that compound the profiles contain volcanic glass between 20 and 90%. The results of two paleosols with different percentage of volcanic glass in the parent material (correlated to Marine Isotope Stage 5, MIS 5) exposed at Corralito I and Lozada, were compared; an important relationship between environmental magnetism signal and volcanic glass content was observed. All the results suggest that there are variations between different paleosols of the same area and age; such variations are attributed to content of volcanic glass in parent material; time of exposure of the parent material to pedogenic processes; and geomorphological place of each profile. At present, it is not possible to quantify certainly the paleo-precipitation index. Only qualitative interpretation can be done taking into account many variables of the geological system.

Keywords: environmental magnetism, mineralogy, past climate

1. INTRODUCTION

Throughout geological history there have been many global warming events entirely natural. Therefore, it is clear that the study of the past record global warming is critical to estimate time and environmental impact of the current warming. The last interglacial interval before this, is called Marine Isotope Stage 5 (MIS 5), is characterized by a general

global warming, similar to present climate conditions (*Siddall et al., 2007*; *Lisiecki and Raymo, 2005*). Studies of the MIS 5 are very scarce in the Southern Hemisphere, particularly in Argentina. Cenozoic deposits are mainly continental in the Chacopampean plain; these deposits constitute a vast sedimentary cover of variable thickness. Pleistocene record is characterized by loessic sediments modified by pedogenic processes (*Zárate, 2003*).

Particularly, the record of the MIS 5 has been reported in only few locations (*Kemp et al., 2006*; *Frechen et al., 2009*). Both contributions identified this stage by luminescence techniques. *Kemp et al. (2006)* identified one representative profile in Baradero (Buenos Aires) and the other one in Lozada (Córdoba Province). *Frechen et al. (2009*) found geological record assignable to the same isotopic stage in Corralito and Monte Ralo, both in Córdoba province.

These eolian continental sediments, loess, have proved to be a good record of climate changes since magnetic properties are an excellent proxy to detect climate change (*Oches and Banerjee 1996*, among others). Currently, there are several hypotheses about the origin of the magnetic signal in paleosols developed on loess (*Evans, 1999, 2001*; *Maher, 1998*; *Boyle et al., 2010*; *Orgeira et al., 2011*). *Maher (1998)* proposed that the soil enhancement transform weakly magnetic iron oxides; these operations are ruled by factors like temperature, soil moisture, redox conditions, organic matter and mainly by bacterial activity. This bacterial activity according to this author may play a key role in the production of ultrafine-grained magnetite. *Evans (1999, 2001)* proposed for the Alaskan loess, the so-called *wind-vigor* model with the greater efficiency of atmospheric entrainment and transport of dense magnetic Fe oxide grains during glacial times, when wind action is maximal, with respect to the less dense (e.g., quartz) non-magnetic minerals. According to this model, glacial sediments contain higher concentrations of magnetic minerals and are more magnetic.

Boyle et al. (2010) proposed that the formation of secondary ferrimagnetic minerals require parent material rich in Fe and that the main control variables are: precipitations and temperature. However, *Orgeira et al. (2011)* suggest that the first amount of Fe minerals is not a first order control on the pedogenic magnetic signal. *Orgeira et al. (2011)* developed a model which incorporated a broader set of climate parameters that influence the processes of formation-destruction of magnetic particles, thus achieving a successful modeling of the magnetic signal. Not only climate parameters are taking into account in this hypothesis also geomorphological aspects such as drainage as was analyzed in *Orgeira et al. (2008)*, who suggested that the differential soil moisture could explain different magnetic signal because drainage seems to be the variable that conditions the process of reduction loss. As well, the formation of pedogenic magnetite is conditioned by soil drainage, intermediate pH, the presence of organic matter and cation exchange capacity. Both, the weathering of iron primary minerals and the neoformation of secondary minerals are affected by the pH/Eh ratio. The rate of magnetite production is proportional to the frequency of drying/moisturizing phases, and to the fraction of wet pores in the soil. The drying/moisturizing frequency is controlled by rainfall, while the fraction of wet pore, which is related to the soil moisture, is controlled by the balance between water input by rainfall and water loss by evapotranspiration. During the drying phase, surface oxidation of pedogenic magnetite produces a maghemite shell whose

growth is controlled by the outward diffusion of Fe^{2+} ions. If a partly oxidized magnetite particle is exposed to reducing conditions during the moisturizing phase, the maghemite shell is dissolved. Maghemitization is thus responsible for the destruction of pedogenic magnetite in an active soil. The destruction rate is proportional to the maghemite shell mass, which depends on the average time interval between rain events, and to the frequency of drying/moisturizing phases.

The frequency of drying/moisturizing cycles let the idea of the existence of a pedogenetic threshold driven by these water balance in the soil, and was used by *Orgeira and Compagnucci (2006, 2010)* to explain the increase and decrease of magnetic signal in the loessial soils of the world. The rainfall and the current evapotranspiration of Córdoba are compensated, it means there is a balance between the generation of pedogenetic magnetite and the loss of magnetic particles, so neither generation nor depletion is expected.

Moreover, *Florindo et al. (2003)* proposed that the loss of magnetite is also influenced by the presence of water with high percentages of dissolved silica; it can generate the dissolution of detrital ferrimagnetic minerals under varied redox and pH conditions. In periglacial loessic deposits with high input of volcanic material, such as the Argentinian ones, the presence of volcanic glass could be a forcing of relevant magnitude in the modulation of the magnetic signal during pedogenetic processes.

The main goal of this study is to compare the geological characteristics and magnetic properties of four profiles in order to clarify how the mineralogy, principally the presence of volcanic glass, would affect or not in quantifying the paleo-precipitation after the *Orgeira's et al. (2011)* hypothesis. This work includes the study of geological record that has been assigned to Marine Isotopic Stage 5 (MIS 5) and the Marine Isotope Stage 3 (MIS 3) reported in marine and ice cores (*Siddall et al., 2007*; *Lisiecki and Raymo, 2005*).

2. GEOLOGICAL SETTING

The studied profiles are situated in the Chacopampean plain, geological province, within the Llanura Pampeana (Pampean plain) sub-province, where two associations can be distinguished: the Depresión Periférica (Peripheral Depression) and the Plataforma Basculada (Tilted Platform) (*Capitanelli, 1979*). The Tilted Platform consists of two sub-associations*:* the Plataforma Basculada Ondulada and the Plataforma Basculada Plana (the Undulated Tilted Platform and the Flat Tilted Platform). These geomorphological areas are conformed by wind-blown sediments (loess) and reworked loess, i.e. water remobilization, it means re-suspension and re-deposition after the primary wind deposition (*Argüello et al., 2012*). The estimated age for these sediments is Pleistocene–Late Holocene. Mineralogically, the Pampean loess contents abundant volcanic glass, quartz and plagioclase (*Teruggi, 1957*; *Muhs and Zárate, 2001*).

The probable source areas are located in SW flood plains and fluvial fans of rivers which drain the Andean glaciers (*Iriondo and Kröhling, 1995*; *Zárate, 2003*); Pampean Ranges from Córdoba and San Luis, and volcanic emissions from the west Mendoza and Neuquén provinces (*Iriondo, 1997*). More recent work suggests three sources areas, Patagonia, W central Argentina and Puna/Altiplano (*Gili and Gaiero, 2014*). Despite these minor differences over the source areas, everyone agrees that W and SW winds are responsible for transporting the material.

Corralito I, Monte Ralo and Lozada profiles are located in the Undulated Tilted Platform, which is conform by elongated rounded hills and ridges with variable slope, between 1% and 3% and heights of around 10 m. It is common rill erosion, both straight and meandering, and in extreme cases, gullies. Corralito II profile is in the Flat Tilted Platform sub-association. This sub-association is characterized by gently rolling hills with a 1% slope, with an approximate age of between 115 and 5 ka (*Frechen et al., 2009*; *Kemp et al., 2006*).

Mean annual temperature ranges between 14 and 17°C, and the irregular distribution of annual precipitation is a typical feature. About 80% of annual rainfall occurs during the austral summer due to humid air coming in from the north (*Pasquini et al., 2006*). Mean annual precipitation for the record period 1960–2015 is 815 mm, which is concentrated between November and April, i.e. the wet season (660 mm for the same record period).

Corralito I (32°0.11′S; 64°11.13′W, 469 m a.s.l.) and Corralito II (32°0.26′S; 64°7.35′W, 433 m a.s.l.) profiles are in a gully of 20 km long and 20–40 m wide, approximately (Fig. 1).

Lozada profile is exposed along an abandoned road excavation on an extensive plain; its coordinates are 31°39′S and 64°8′W, 490 m a.s.l. (Fig. 1).

The Monte Ralo gully is at the head of the basin that is called Cortada de Grasso and extends over flat loess hills. The coordinates of Monte Ralo profile are: 31°54′S and 64°10′W, 496 m a.s.l. (Fig. 1).

3. MATERIALS AND METHODS

The studied sequence can be considered a sedimentary-pedological succession as described by *Freytenet (1971)*. Discontinuities on sedimentation were identified; they were represented by erosion surfaces. Once the discontinuities were established, the units were defined regarding thickness, bed geometry, color, sedimentary and pedogenic structures, degree of consolidation, particle size parameters and composition. Color determination was made using the Rock Color Chart Committee chromatic standards. The profiles were measured, and samples weighing 500 g were taken. Particle size and calcium carbonate content were determined in bulk samples at vertical intervals of approximately 50 cm, using a laser diffraction particle analyzer (CILAS) and a Sheibler calcimeter (*Gale and Hoare, 1992*), respectively. Both devices were available at the Geology Department of Buenos Aires University. Results were expressed as mean for grain size and as percentage for calcium carbonate content.

X-ray analysis of the clay fraction was made on selected samples, and it was performed on a Philips diffractometer, Model X'pert with Cu radiation with graphite monochromator belonging to SEGEMAR (Geological Argentine Mining Service).

Representative samples of each horizon were chosen for the mineralogical analysis of sands. In the selected samples, cements were destroyed and the material was dispersed by ultrasound. After sieving the samples, fractions between 100 and 50 μm were studied. The mineralogical studies were carried out using polarized microscopy on 1000 grains, following *Karlsson (1990)* methodology.

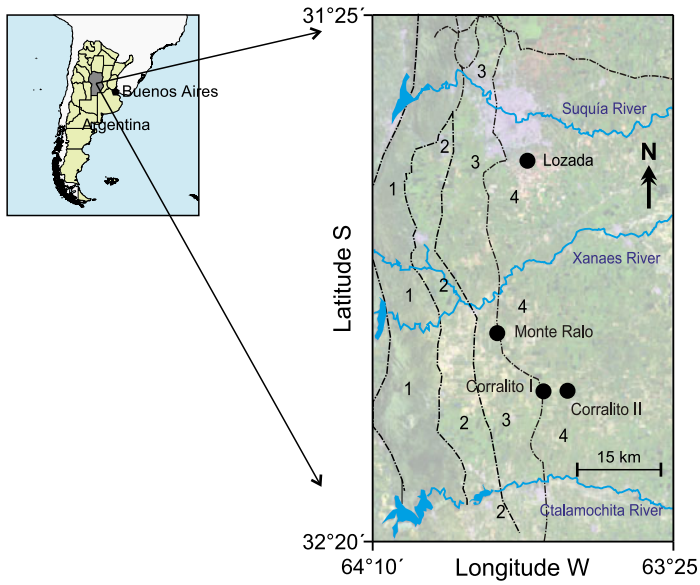

Fig. 1. Location of the studied profiles. 1 - Córdoba Range, 2 - Peripheral Depression, 3 - Undulated Tilted Platform, 4 - Flat Tilted Platform..

Optically stimulated luminescence (OSL) ages of two samples from Corralito II profile were obtained. Samples were taken according to the Luminiscense Dating Laboratory of Illinois at Chicago protocol, where the samples were sent for analysis. The principles of the technique are detailed in *Forman et al. (2000).*

Two samples from Corralito I profile were taken and dated by ^{14}C chronology, specifically Accelerated Mass Spectrometry (AMS). The samples were taken from the top and the base of Bt horizon from the buried soil. The samples were sent to the Accelerator Mass Spectrometry Laboratory at the University of Arizona. The calibrations of the results were performed with SHCal04.14c (*McCormarc et al., 2004*) in conjunction with Calib program (*Stuiver and Reimer, 1993*).

4. RESULTS

In order to facilitate the reader's understanding of this contribution, all profiles are described from base to top.

4.1. Corralito I

The profile is integrated by five units with the following characteristics.

Unit A

Main features. This unit has 2.1 m of thickness; the geometry of the base corresponds to pale pink color (5YR 7/3) sediments, friable, with 6% of calcium carbonate in the mass

and concretions of 1 cm in diameter. The average grain size is medium to coarse silt, while sand and clay fractions do not exceed 10%. Pedological features are scarce in the basal and middle sections, but become relevant in the upper 0.4 m of the unit, which can be observed a prism structure, structural evidence like pores and empty spaces left by roots. Its color is pink (5YR 7/4) (Fig. 2). This unit corresponds to the Paleosol III.

Mineralogical composition. Quartz and plagioclase are the dominant minerals, followed by clays, mainly illite- smectite. It has traces of calcite and chlorite (Table 1). Regarding the percentage of volcanic glass is 40% at its base and 20% on the top (Table 2).

Environmental Magnetism. Total magnetic susceptibility X_{total} shows an increase in the upper 40 cm from the basal section. The extensive parameters, saturation magnetization (M_S) and remanent saturation magnetization (M_{rs}) are highly fluctuating. Magnetic mineralogy for this section indicates Ti-magnetite and magnetite as indicated the coercivity (H_c) and remanent coercivity (H_{cr}); (Fig. 6 later). The different kinds of magnetic grain size is mainly pseudo-single domain (PSD) with minor percentage of superparamagnetic grains (SP) (*Rouzaut et al., 2012, 2015*).

Unit B

*Main features.*This unit has 2.9 m thick, the base is constituted by a friable sediment, reddish-yellow (5YR 7/6) color, with massive structure and 2% of calcium carbonate. The average size of sediments corresponds to medium to fine silt; sands and clays values remain under 10%.The top of the unit, has a thickness of 1.9 m and corresponds to sediment that has abundant pores with pedogenic features and structural cracks. Its color is pink (5YR 8/4) (Fig. 2). This unit is represented by paleosol II.

Mineralogical composition. It is dominated by quartz and plagioclase with minor amounts of alkali feldspar. Clay minerals form, on average, up to 30% of the total content, while minor components as cristobalite or hematite are present as traces in some samples. Calcite appears with variable contents, but always less than 10%. The main clays in these samples are illite-smectite (Table 1). The percentage of volcanic glass ranges between 30% in the base and 60% at the top (Table 2).

Environmental Magnetism: The X_{total} does not show notable changes. The extensive parameters, M_{rs} and M_S, are highly variable. The magnetic mineralogy is similar to the unit A, it indicates Ti-magnetite and magnetite (Fig. 6 later). The magnetic grain size is PSD (*Rouzaut et al., 2012, 2015*).

Unit C

Main Features. This unit has 2.4 m height; its base consists on friable sediments, pink (5YR 7/4) color, with a massive structure and 2–4% of calcium carbonate dispersed in the matrix. It presents interbedded lenticular bodies of 1 m thickness and 1 m long, of pink (5YR 8/4) color, very hard and compact; it breaks into angular blocks. The average size of the sediments correspond medium to coarse silt. Sand and clay hold values less than 10%. Pedological features are scarce in the basal and middle sections, but become relevant in the last 160 cm, formed by a friable material of light reddish brown (5YR 6/3) color with prismatic structure and structural pores, with the presence of rhizoliths (Fig. 2). This unit corresponds to Paleosol I.

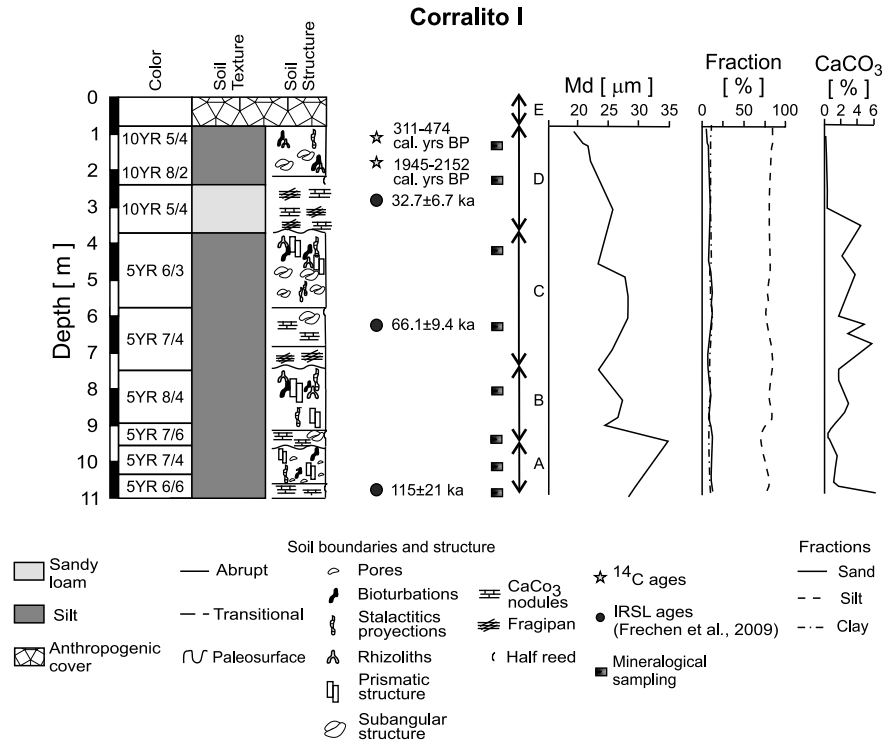

Fig. 2. Corralito I stratigraphic profile. Color is expressed using Munsell soil color codes (*Munsell, 1912*). *Md*: average grain size.

Mineralogical composition. Quartz is between 25% and 30% of abundance, more or less similar to the plagioclase, which also reaches a maximum of 40% on the samples. Alkali feldspar levels are much lower, reaching only exceptionally 15%, and the global values with an average of about 10%. There is a high content of smectite clays, between 40–45% (Table 1). The percentage of volcanic glass, both in its base and top, remains at 20% (Table 2).

Environmental Magnetism. The X_{total} shows a slight decrease in the upper section than in the base. The extensive parameters, M_{rs} and M_s are highly variable. The magnetic mineralogy is similar to the A and B units and indicates Ti-magnetite and magnetite (Fig. 6 later). The magnetic grain size is PSD (*Rouzaut et al., 2012 and 2015*).

Unit D

Main features. This unit is 2 m thick, on its base is observed 0.25 m of sediment cover with numerous cracks that give a concrecional appearance and in which has been introduced calcium carbonate (2%). It is erosively cut by a lens of 6 m length and 0.35 m thickness, with fine stratification and lamination composed of very fine sand and silt brownish yellow (10YR 5/4) color. Sedimentary structures correspond to tabular cross-

Table 1. X-ray diffraction data of the Corralito I profile (data in %). Tr.: trace amount.

	Unit A	Unit B		Unit C		Unit D	
Depth of sampling [cm from the base]	120	250	300	600	710	1040	1050
Bulk Sample							
Quartz	40	25	25	30	25	30	40
Plagioclase	20	25	35	40	30	40	35
K-feldespar	15	15	15	10	15	10	10
Clays	25	35	20	20	30	20	15
Calcite	Tr.	Tr.	5	--	Tr.	--	Tr.
Cristobalite	---	Tr.	Tr.	--	Tr.	--	--
Others				Tr.		Tr.	Tr.
Clays							
Illite (Illite/Smectite)	65	70	55	60	65	55	60
Smectite	35	30	45	40	35	45	40
Chlorite	Tr.	Tr.	<5	Tr.	Tr.	<5	Tr.

Table 2. Volcanic glass in the units of the Corralito I profile.

Unit	Position	Depth of Sampling [cm from the base]	Estimated Volcanic Glass [%]	Others [%]
D	Top	980	30	70
	Base	870	40	60
C	Top	670	20	80
	Base	550	20	80
B	Top	300	60	40
	Base	170	30	70
A	Top	80	20	80
	Base	20	40	60

bedding and low flow rate. The top of the lens is represented by silt. The grain size of sediments corresponds to medium to fine silt. Sands and clays values remain under 10%. At the top, 0.6 m of silty material is present with many voids and poorly defined prismatic structure. Then 0.8 m of clay sediments is observed, also with tabular geometry, light gray (10YR 7/1) color, with probable nests molds and bioturbation structures (Fig. 2). This unit is represented by the buried soil.

Mineralogical composition. The unit D has plagioclase as a dominant mineral, followed in importance by quartz, 30–35% and 10% orthoclase, with traces of calcite. The percentage of clay is low, between 10–15%, predominantly illite (Table 1). Volcanic glass is observed and it is 40% in the base and 30% at the top (Table 2).

Environmental magnetism. The X_{total} shows a slight increase in the upper segment compared to base segment. The extensive parameters, M_{rs} and M_s are highly variable. The magnetic mineralogy is similar to the A, B and C units and indicates Ti-magnetite and

magnetite and hematite (Fig. 6 later). The size of the magnetic mineralogy is PSD (*Rouzaut et al., 2012 and 2015*).

Unit E

Main features. In erosional unconformity a deposit of 0.80 m is observed in the sampling area, conformed by silt, sand and fine gravel of fluvial origin with residues of human activity.

4.2. Corralito II

The profile is integrated by five units described by the following characteristics.

Unit A

Main features. In the base of the profile 3.2 m of reddish-brown (5YR 5/4) color sediment is observed, characterized by cross-bedding structures interbeded with horizontal lamination. Then a 20 cm of imbricated clasts structure is observed and it is compound by 1 to 2 cm of silty intraclasts. The grain size average indicates, for this unit, fine to coarse silt; the finest sediments are in the center of the unit and the thickest at the base and at the top. The percentage of calcium carbonate also has a large fluctuation between 1–3% (Fig. 3). This unit is formed by fluvial sediments.

Mineralogical composition. The samples are dominated by quartz and plagioclase, with minor amounts of alkali feldspar. Clay minerals include 25% of the total content, while minor components as cristobalite or hematite are present as traces in some samples. Calcite appears with variable contents, but always less than 10% and generally in trace amounts. It is observed in the total samples, cristobalite traces. The dominant clays in this unit are smectite and illite-smectite with less amounts of chlorite (Table 3).

Environmental magnetism. The X_{total} and the extensive parameters, M_S and M_{rs} are highly variable around the analyzed section. The magnetic mineralogy indicates Ti-magnetite and magnetite (Fig. 6 later). The magnetic grain size is PSD (*Rouzaut et al., 2015*).

Unit B

Main features. This unit consists of a brown (7.5YR 4/4) color sediment of 4.4 m thickness, friable, with abundant $CaCO_3$ concretions of 1 cm diameter. The average grain size of the sediments corresponds to medium to coarse silt. Pedological features are scarce in the basal and middle section, but become relevant in the last 0.5 m of the unit, where is observed a reddish-brown (5YR 5/4) color sediment, slightly resilient with a strong, subangular block structure and clay-skins on the faces of the aggregates. The top of this unit presents rhizoliths (Fig. 3). This section is represented by Paleosol III.

Mineralogical composition. In unit B, quartz and plagioclase are the dominant minerals with 30%. Alkali feldspar content reaches 15% and clays join 20% of the total amount, being the dominant clay the illite-smectite and then the smectite (Table 3). The percentage of volcanic glass remains at 20% for the base and 40% for the top (Table 4).

Environmental magnetism. The X_{total} shows an increment in the upper segment compared to base of the unit. The extensive parameters, M_S and M_{rs}, are highly variable. The magnetic mineralogy is similar to the A unit and indicates Ti-magnetite and

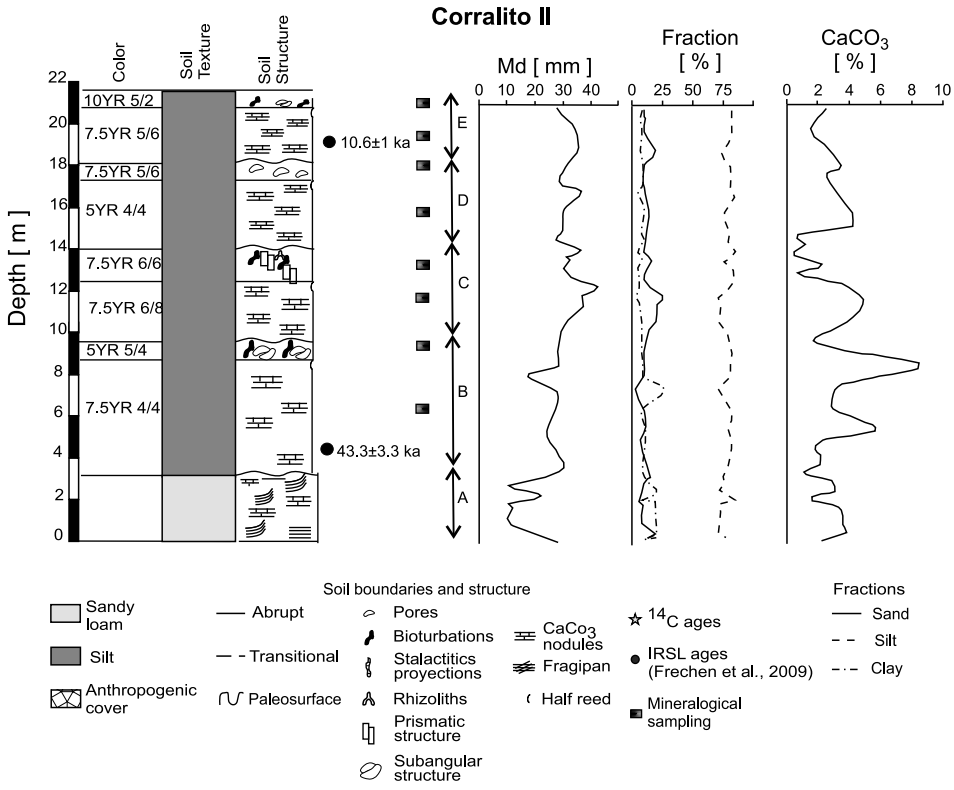

Fig. 3. Corralito II stratigraphic profile. Color is expressed using Munsell soil color codes (*Munsell, 1912*). *Md*: average grain size.

magnetite (Fig. 6 later). The magnetic grain size indicates the presence of PSD (*Rouzaut et al., 2015*).

Unit C

Main features. This unit is made up of 2.6 m of reddish yellow (7.5YR 6/8) color sediment with abundant calcium carbonate concretions (1–4%). The average grain size of the sediments corresponds to medium to coarse silt. This sediment gradually moves to reddish yellow (7.5YR 6/6) color material, of 1.8 m thickness with a strong prismatic structure and pedogenetic characteristics (Fig. 3). This unit corresponds to Paleosol II.

Mineralogical composition. The composition of the C unit is similar to the previous one, without major changes in the quartz, plagioclase and orthoclase percentages. Clays also constitute 20% of the total sample, but in this case the smectite has 35%, slightly higher than the previous unit content, however illite-smectite remains the dominant clay (Table 3). The volcanic glass percentage is maintained at 50% for the base and 40% for the top (Table 4).

Table 3. X-ray diffraction data of the Corralito II profile (data in %). Tr.: trace amount.

	Unit A		Unit B	Unit C	Unit D	Unit E
Depth of sampling [cm from the base]	60	160	740	1130	1460	2030
Bulk sample						
Quartz	35	25	30	30	35	35
Plagioclase	30	20	30	30	25	30
K-feldespar	10	15	15	15	15	15
Clays	25	30	20	20	25	20
Calcite	Tr.	10	5	5	Tr.	Tr.
Cristobalite	Tr.	Tr.	Tr.	Tr.	Tr.	Tr.
Others						
Clays						
Illite (Illite/Smectite)	70	70	55	65	50	60
Smectite	25	25	40	35	45	35
Chlorite	5	5	5	Tr.	5	5

Table 4. Volcanic glass in the units of the Corralito II profile.

Unit	Position	Depth of Sampling [cm from the base]	Estimated Volcanic Glass [%]	Others [%]
E	Top	2080	40	60
	Base	1970	10	90
D	Top	1820	40	60
	Base	1590	50	50
C	Top	1300	40	60
	Base	1190	50	50
B	Top	910	40	60
	Base	650	20	80
A	Fluvial			

Environmental magnetism. The X_{total} presents a significant depletion in the upper part of the unit compared to base. The extensive parameters, M_s and M_{rs}, are highly variable. The magnetic mineralogy indicates hematite (Fig. 6 later). The kinds of magnetic grain size are PSD and single-domain–multi-domain (SD-MD) (*Rouzaut et al., 2015*).

Unit D

Main Features. In this unit a layer of silty sediment of 3.2 m, brittle, reddish brown (5YR 4/4) color is observed. At the top of the unit 0.6 m of shiny brown (7.5YR 5/6) color and porous sediment is detected. It has a moderately resistant block structure. The average grain size for this unit ranges between 25 and 30 μm (medium silt). The percentages of calcium carbonate grow from the base to the middle sector of the unit, the values are between 1 and 4% (Fig. 3). This unit is represented by Paleosol I.

Mineralogical composition. The D unit is dominated by quartz and plagioclase (35 and 25%, respectively). Orthoclase forms 15% of the sample and clay content constitutes 25% of total. Only trace amounts of calcite and cristobalite are found. The clays which dominate this unit are illite-smectite and smectite (Table 3). The percentage of volcanic glass ranges between 50% at the base and 40% at the top (Table 4).

Environmental magnetism. The X_{total} presents a significant depletion in the upper part of the unit than in the base. The extensive parameters, M_s and M_{rs}, are highly variable. The magnetic mineralogy indicates Ti-magnetite and magnetite (Fig. 6 later). The kinds of magnetic grain size are PSD and SD-MD (*Rouzaut et al., 2015*).

Unit E

Main features. This unit is made up of 3.5 m of a friable and massive sediment, with 2.5% of calcium carbonate in the mass, shiny brown (7.5YR 5/6) color. The main average grain size of the sediments corresponds to medium silt. Pedological features are scarce in the basal and middle part of the unit, but become relevant in the last 0.5 m and are constituted by Bw and Ap horizons that conform the present cultivated soil (Fig. 3).

Mineralogical composition. Quartz is the dominant mineral with a 35%, plagioclase with 30% and ortosa remaining 15%. Clays still form 20% of the total sample and the dominant fractions are illite-smectite (Table 3). The percentage of volcanic glass remains at 10% for the base and 40% for the top (Table 4).

Environmental magnetism. The X_{total} presents a significant increment in the upper part of the unit than in the base. The extensive parameters, M_s and M_{rs}, are highly variable. The magnetic mineralogy indicates Ti-magnetite and magnetite (Fig. 6 later). The kinds of magnetic grain size are PSD and SD-MD (*Rouzaut et al., 2015*).

4.3. Monte Ralo

This profile is composed of three main units with the following features.

Unit A

Main features. The base of this unit has thickness of 0.3 m and is represented by light brown (7.5YR 6/4) color sediments with massive calcium carbonate (between 2–4%). The main average grain size is medium silt and forms 75% of the total sediment. Pedological features are scarce in the basal and middle section of the unit, but become relevant in the last 0.4 m of the top of the unit; they are sediments of light brown (7.5YR 6/4) color, which presents stalactites projections and many structural pores of 1–3 cm diameter, with bioturbation and clay-skins (Fig. 4). This unit is represented by Paleosol I.

Mineralogical composition. The unit A is dominated by quartz and plagioclase, with minor amounts of alkali feldspar. Quartz is 30% more or less similar to the plagioclase abundance, which also reaches 25%. Alkali feldspar levels are much lower, reaching 15%. The minerals that seem as traces are hematite, which never exceeds 1% but is presented in almost all samples, and occasionally cristobalite (perhaps product of devitrification). Clay minerals, illite (with some participation of illite-smectite with poor expandable layer) and smectite with very poor quality of crystallization. It is possibly that smectite is a product from volcanic glass alteration (Table 5). The percentage of volcanic glass is 50% for the base and 70% for the top (Table 6).

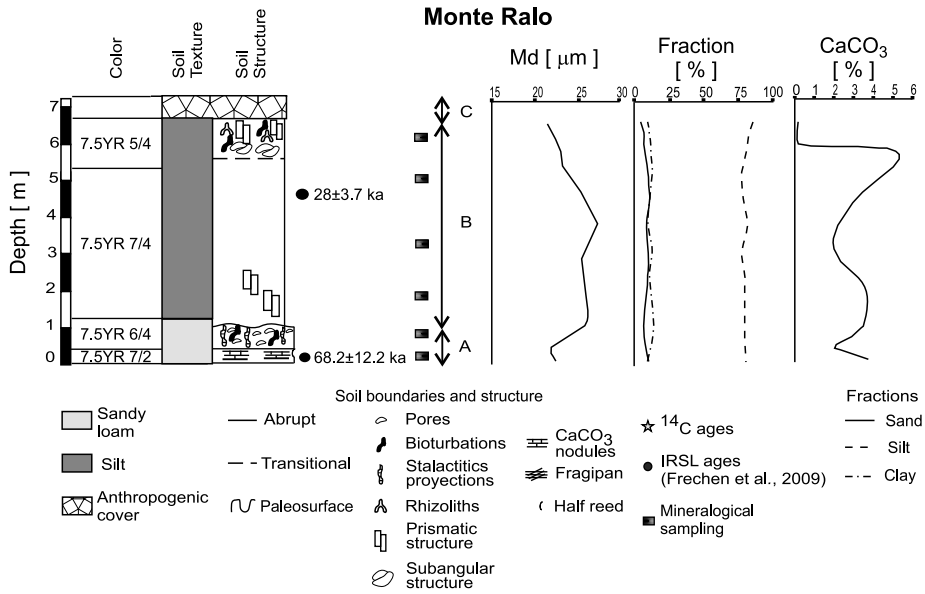

Fig. 4. Monte Ralo stratigraphic profile. Color is expressed using Munsell soil color codes (*Munsell, 1912*). *Md*: average grain size.

Environmental magnetism. The X_{total} presents a significant increment in the upper part of the unit than in the base. The extensive parameters, M_s and M_{rs}, are highly variable. The magnetic mineralogy indicates Ti-magnetite and magnetite; hematite seems to be masked in analysis of magnetic properties (Fig. 6 later). The magnetic grain size is PSD (*Rouzaut et al., 2013*).

Unit B

Main features. The unit B overlies net contact to unit A; it has 4.7 m thickness. The reworked loess deposit has tabular geometry, they are massive, pink (7.5YR 7/4) color with calcium carbonate in the mass (3–5%). The average grain size is medium silt. Pedological features are scarce in the basal and middle section of the unit, but become relevant at the top of brown (7.5YR 5/4) color sediments; they constitute the Bwb and Ab horizons and form a buried soil (Fig. 4).

Mineralogical composition. The mineralogical analysis for the unit B indicates that quartz is the main mineral with 35%, followed in abundance with plagioclase and orthoclase ranging between 30–10%. The analysis by X-ray diffraction, exposes that the clay minerals are 25% from the total sample and consist primarily of illite and illite-smectite with traces of chlorite (Table 5). The percentage of volcanic glass is 50% for the base, between 10–25% for the middle sector and, 25% for the top (Table 6).

Environmental magnetism. The X_{total} presents a significant raise in the upper part of the unit than in the base. The extensive parameters, M_s and M_{rs}, are highly variable. The

Table 5. X-ray diffraction data of the Monte Ralo profile (data in %). Tr.: trace amount.

	Unit A	Unit B
Depth of sampling [cm from the base]	80	660
Bulk Sample		
Quartz	30	35
Plagioclase	30	30
K-feldespar	15	10
Clays	25	25
Calcite	Tr.	Tr.
Cristobalite	Tr.	Tr.
Others		
Clays		
Illite (Illite/Smectite)	75	70
Smectite	25	25
Chlorite	Tr.	5

Table 6. Volcanic glass in the units of the Monte Ralo profile.

Unit	Position	Depth of Sampling [cm from the base]	Estimated Volcanic Glass [%]	Others [%]
B	Top	620	25	75
	Middle	510	25	75
	Middle	330	10	90
	Base	190	50	50
A	Top	90	70	30
	Base	50	50	50

magnetic mineralogy indicates Ti-magnetite and magnetite (Fig. 6 later). The magnetic grain size is PSD (*Rouzaut et al., 2013*).

Unit C

Unit C corresponds to a variable thickness (0.5–0.8 m) layer, consisting of silt and fine sand with anthropogenic waste materials (Fig. 4).

4.4. Lozada

The profile is composed of three main units with the following characteristics.

Unit A

Main features. It is constituted of a sediment of 1 m thickness, friable, dark yellowish brown (10YR 4/4) color, with 5% calcium carbonate in the mass. The average grain size of the sediments corresponds to medium to coarse silt. Pedological features are scarce in the basal and middle sector of the unit; however, they are common in the sediments at the top. This last meter is represented by brown (7.5YR 4/4) silty loam sediment, in where

there is evidence of bioturbation and clay translocation (Fig. 5). This unit is conformed by Paleosol I.

Mineralogical composition. The mineralogical analysis for the unit A indicates that quartz is the main mineral, followed in abundance by plagioclase and orthoclase The analysis by X-ray diffraction, exposes that the clay minerals are illite and illite-smectite (*Muhs and Zárate, 2001*). The percentage of volcanic glass for the base of this unit is 20% and 95% at the top (Table 7).

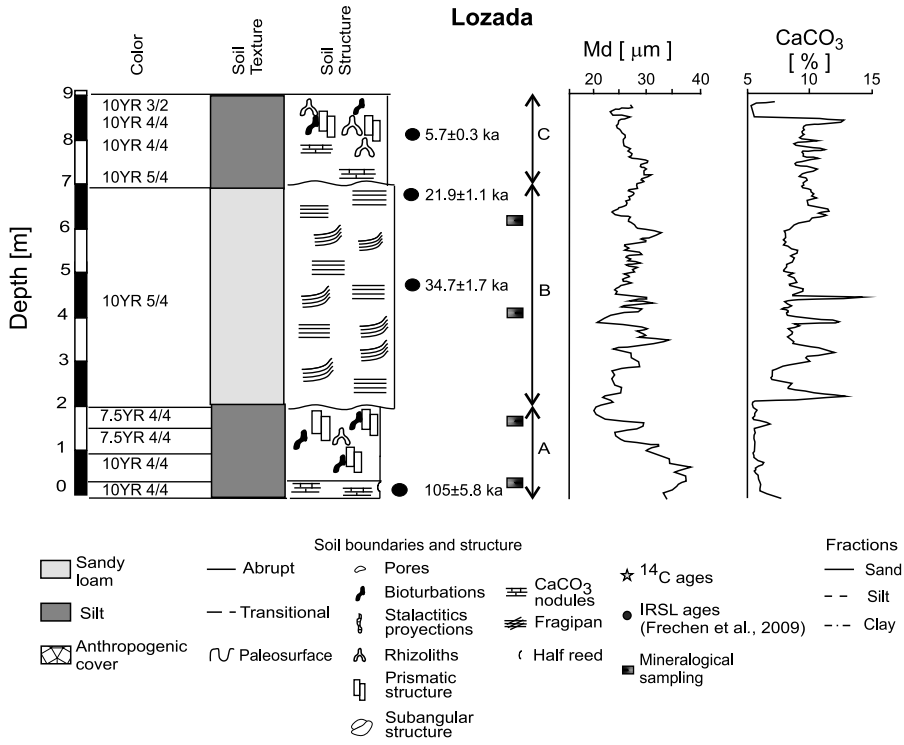

Fig. 5. Lozada stratigraphic profile. Color is expressed using Munsell soil color codes (*Munsell, 1912*). *Md*: average grain size.

Table 7. Volcanic glass in the units of the Lozada profile.

Unit	Position	Depth of Sampling [cm from the base]	Estimated Volcanic Glass [%]	Others [%]
C	Top	---	---	100
	Base	---	40	60
B	Top	620	5	95
	Base	410	10	90
A	Top	180	95	5
	Base	50	20	80

Environmental magnetism. The X_{total} presents slight depletion in the upper part of the unit than in the base. The extensive parameters, M_s and M_{rs}, are highly variable. The magnetic mineralogy indicates Ti-magnetite and magnetite. The magnetic grain size is PSD (*Rouzaut et al., 2013*) (Fig. 6).

Unit B

Main features. This unit consists of 4 m of yellowish brown (10YR 5/4) color sediment, with horizontal and subhorizontal lamination and subrounded clasts. These clasts present clay-skins which allow us to infer that would come from pedogenic sediments. The particle grain size for this unit is highly variable, but always it remains in the range of coarse silt. The carbonate percentages range between 5 and 15% (Fig. 5).This unit is represented by reworked loess.

Mineralogical composition. The mineralogical analysis for the unit B indicates that quartz is the main mineral followed in abundance by plagioclase and orthoclase. The analysis by X-ray diffraction, exposes that the clay minerals are illite and illite-smectite (*Muhs and Zárate, 2001*). The percentage of volcanic glass in the base of the unit is 10% and at the top is 5% (Table 7).

Environmental magnetism. The extensive parameters are highly variable; indicate fluctuation in the concentration of magnetic minerals. The magnetic mineralogy indicates Ti-magnetite and magnetite (Fig. 6). The kinds of magnetic grain size are PSD and SD-MD (*Rouzaut et al., 2013*).

Unit C

Main features. This unit is the present soil; it is a Typical Haplustoll with the following profile A-Bw-BCk-Ck. The A horizon is very dark grayish brown (10YR 3/2) color, silty loam texture; Bw horizon is yellowish dark brown (10YR 4/4) color and has bioturbation evidence and emerging clay-skins; BCk horizon is dark yellowish brown (10YR 4/4) color and there is abundant calcium carbonate in the mass. Finally Ck is yellowish brown (10YR 5/4) color and is massive (Fig. 5). This unit is represented by the present soil.

Mineralogical composition. The mineralogical analysis for the unit C indicates that quartz is the main mineral followed in abundance with plagioclase and orthoclase. The analysis by X-ray diffraction exposes that the clay minerals are illite and illite-smectite with traces of chlorite (*Muhs and Zárate, 2001*). The mineralogical analysis of the present soil indicates 40% of volcanic glass for parent material and 0% for the top of the soil (Table 7).

Environmental magnetism. Such as the previous unit described, the extensive parameters are highly variable suggesting fluctuation in the magnetic minerals. In that case, slight increment is observed toward the top of the unit. The magnetic mineralogy indicates Ti-magnetite and magnetite (Fig. 6). The kinds of magnetic grain size are PSD and SD-MD (*Rouzaut et al., 2013*).

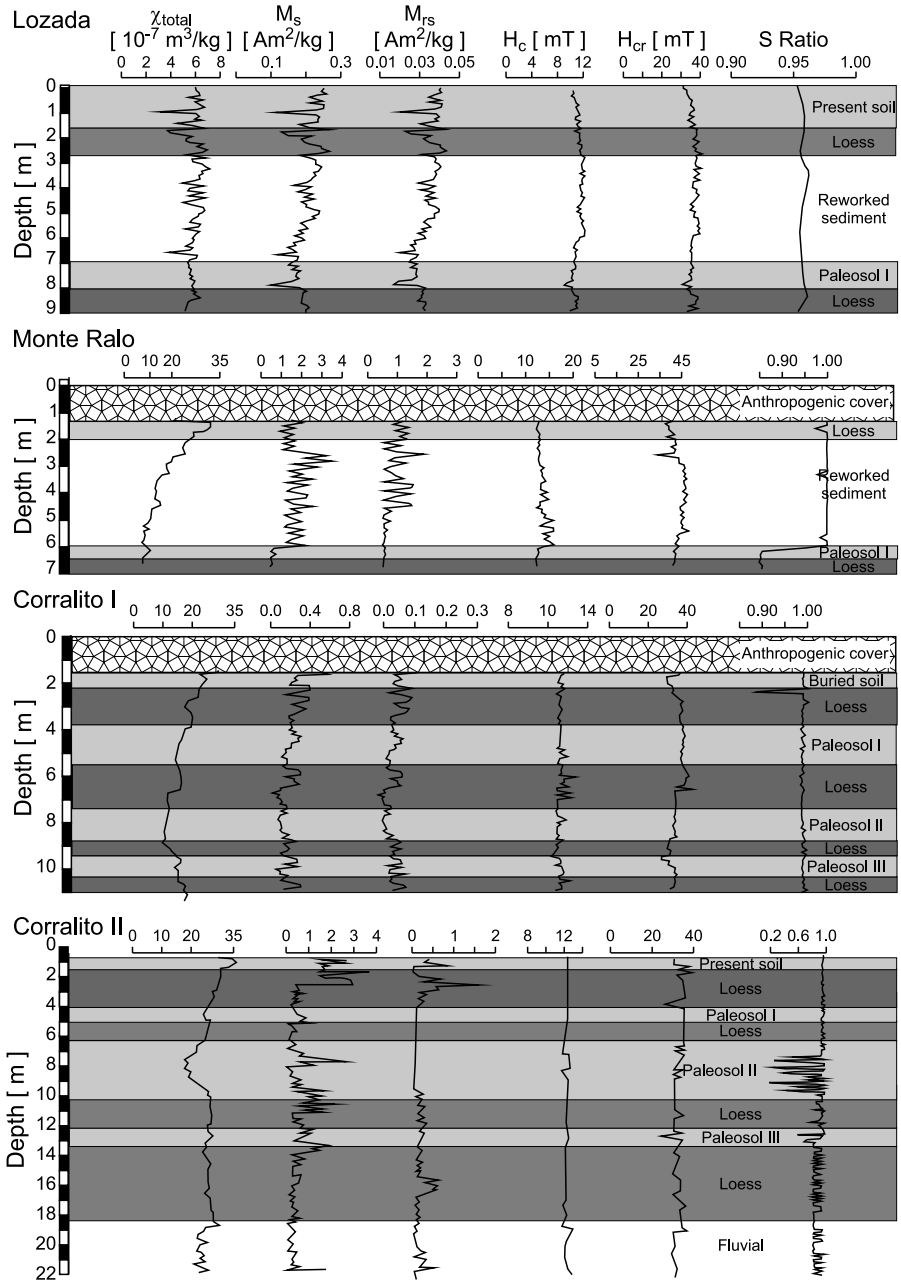

Fig. 6. Magnetic properties of Lozada, Monte Ralo and Corralito I and II profiles. X_{total} - total magnetic susceptibility, M_s - saturation magnetization, M_{rs} - saturation remanent magnetization, H_c – coercive force, H_{cr} - coercivity of remanence, (modified from *Rouzaut et al., 2012, 2013, 2015*).

5. DISCUSSION

According to the luminiscence dating a lithostratigraphic correlation can be made between the four profiles. As reported by *Frechen et al. (2009),* Paleosol II and III from Corralito I (age of the underlying loess, 115 ka) and Paleosol I from Lozada (age of the underlying loess, 105 ka, *Kemp et al., 2006*) represent the same lapse corresponding to Marine Isotope Stage 5, MIS 5 (Fig. 7). Paleosol I from Corralito I (age of the underlying loess, 66.1 ± 9.4 ka, *Frechen et al., 2009*) correlates with the Paleosol III from Corralito II (43.4 ± 3.3 ka; *Rouzaut, 2015)* and Paleosol I from Monte Ralo (68.2 ± 12.2 ka, *Frechen et al., 2009*) (Fig. 7). Paleosols are in the same climatic interval which corresponds to MIS 3. The development of Paleosol I from Corralito I, the Paleosol III from Corralito II and Paleosol I from Monte Ralo confirm the climate improvement suggested by *Kröhling and Carignano (2014).* This period was characterized by a humid climate with fluvial activity and pedogenesis inside the basin. The buried soil at Corralito I (1945–2152 cal. yrs. BP; *Rouzaut, 2015*) and Monte Ralo (28 ± 3.7 ka, *Frechen et al., 2009*), the present soil in Corralito II (10.6 ± 1 ka, *Rouzaut, 2015*) and the present soil in Lozada (5.7 ± 0.3 ka*, Kemp et al., 2006*) correlate with each other, and correspond to the MIS 1, Late Holocene (Fig. 7). The presence of calcium carbonate in all the profiles and illuviation in the Bt horizons in the profiles show similar climatic conditions, with contrasting seasons. The decarbonatation-carbonatation needs a wet period to dissolve and a dry period to precipitate. The illuviation needs a dry period to open the cracks and later coat them with clays; during the wet period in which the crack closes and the clay mobilizes into the pores and sticks forming the cutans. The paleosols do not have an A horizon because they were eroded, anyway it is presumed that melanization took place.

As a first hypothesis, it can be consider that the percentage of volcanic glass found in laboratory analysis could be representative of the original content.

Similarities and differences can be established among the profiles according to the lithostratigraphic comparison. Among the similarities, we can mention that the profiles are mainly loess and reworked loess sequences with pedogenesis in discrete sectors. The general grain size of the sediments (between 70 and 80%) is medium to coarse silt (*Argüello et al., 2012*) (Fig. 7), which indicates a main wind-blown origin (loess and reworked loess, *Argüello et al., 2012*). In the case of Corralito II*,* fluvial sediments, *sensu lato* can be found; they are attributed to ephemeral water courses. This indicates a cyclic and complex sedimentation. Paleosols indicate stability periods of no sedimentation and relatively more humid climatic conditions. The absence of the upper horizons (A), which could be a result of erosion (*Imbellone, 2011*), oxidation (*Kemp, 2001*), or due to the change from wetter to drier climatic conditions (*Kröhling and Carignano, 2014*). However, the presence of bioturbation and rhizoliths show that pedogenic processes were active during sedimentation. The pedological processes inferred in the profiles were similar to the deduced ones in the present soils, those observed in Corralito II and Lozada: these properties are carbonatation-decarbonatation, melanization and clay illuviation, in that order. The development of these processes need contrasting climates stations, i.e. differences in rainfall between the winter and summer periods (*Pasquini et al., 2006*). The

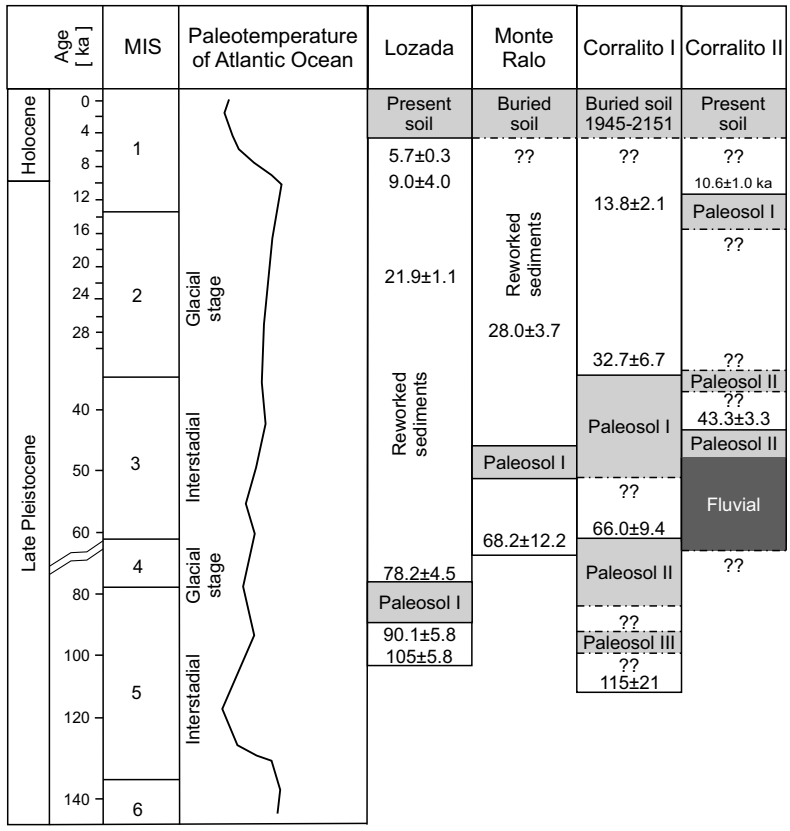

Fig. 7. Lithochronological correlation between the analyzed profiles and their comparison with the Atlantic paleotemperature variation during the Late Pleistocene-Holocene (based on δO^{18} data, *Lisiecki and Raymo, 2005*). MIS - marine isotope stage.

wet period is required for the decarbonatation and the illuviation (clay mobilization); the dry period allows the carbonate and clays precipitate.

The mineralogical composition is mainly quartz, feldspar, plagioclase, and abundant volcanic glass. These mineralogical characteristics, plus the presence of volcanic glass (Fig. 3) in the studied profiles, indicate SW winds and as source area the Andean region, as was already mentioned by previous authors.

The presence of illite, smectite and illite-smectite in all the profiles is in agreement with earlier observations of *Argüello et al. (2012)*. The presence of illite indicates igneous and metamorphic contribution from Pampean Ranges. Furthermore, an increment of illite in older paleosols, is associated with a decrease of smectite due to smectite becomes illite as a result of burial through intermediate stages. Smectite would also be a result of devitrification of volcanic glass present in the parent material. It means that the presence and abundance of smectite indicates the incidence and intensity of weathering processes.

Among the differences detected, it was observed that Corralito II (21 m) profile development is thicker than Corralito I (11 m); even though they are in the same gully and less than 6 km apart. The difference in this development of the profile is caused by the retrogradade erosion characteristic in gullies. According to this premise, Corralito II was first exposed than Corralito I. However, the paleosols thicknesses are higher in Corralito I (Fig. 2) than in Corralito II. The difference in paleosols thickness may be related to the different geomorphological place of the profiles, which produces differences in water infiltration and disparity in the paleosols horizons development. Corralito I is situated in the undulated tilted platform where water concentrates and infiltrates more; Corralito II is in the flat tilted platform where the lower slope causes less water infiltration, so the paleosols thicknesses decrease (Fig. 2).

The magnetic properties (Fig. 6) analysis indicates similarities in the magnetic mineralogy in the studied profiles; magnetite and Ti-magnetite (poor Ti) were detected; hematite was only perceived in discrete sectors of Corralito I, II and Monte Ralo (*Rouzaut et al., 2012, 2013, 2015).* The magnetic mineral grain size indicates mainly presence of pseudo-single domain (PSD), with minor concentration of single domain (SD) and multidomain (MD) (*Rouzaut et al., 2012, 2013, 2015*). This mixture of magnetic grain size reinforces the idea that sediments have been reworked in some sections. However, the magnetic signature does not behave similar between the homologous paleosols ages.

All qualitative observations made about the magnetic signal are carried out with respect to those of the overlying parent material (loess or reworked loess).

Comparison of the magnetic behavior of paleosols assigned to marine isotope stage 5 (MIS 5) allows the following comments. As it can see in Table 8 and Fig. 6, Paleosol I from Lozada shows slight decrease in the extensive magnetic parameters such as susceptibility (X_{total}). In contrast, in the Paleosol III from Corralito I an increment is perceived in the magnetic signal and Paleosol II of the same profile remains unchanged. It suggests for records of same age a slight loss, gain or preservation of the magnetic mineralogy during pedological processes. However, the magnetic mineralogy is the same in the three paleosols. Depletion of magnetic minerals in Paleosol I from Lozada could have been promoted by enriched water silica (*Florindo et al., 2003*); according to the mineralogical analysis 95% of volcanic glass was found in the Paleosol I from Lozada. All this promotes a magnetic depletion. However, in Paleosols II and III from Corralito I, with 60 and 20% of volcanic glass content respectively, a discrepant magnetic behavior was observed. Apparently there is a relationship in these cases with the content of volcanic glass.

The paleosols which have been assigned to MIS 3, i.e. Paleosol I from Corralito I, Paleosol III from Corralito II and Paleosol I from Monte Ralo, showed another forcing in the magnetic signal. The extensive magnetic parameters such as susceptibility (X_{total}) for Paleosol I from Corralito I indicates a slight depletion of magnetic minerals; Paleosol III from Corralito II and Paleosol I from Monte Ralo, show a slight gain of these minerals (Table 8). The magnetic mineralogy indicates the presence of magnetite and Ti-magnetite for all the mentioned paleosols. It is clear that no direct correlation with the content of volcanic glass and magnetic signal is observed. Somehow, other factors are prevailing in the system. Monte Ralo bottom section shows evidence of strong oxidation (see S ratio $S = IRM_{-0.3\,\mathrm{T}} / SIRM$, Fig. 6) indicating a prolonged exposure of Paleosol I to

Table 8. Comparison of key magnetic properties of the marine isotope stages MIS 5, MIS 3 and MIS 1 (arrows indicate gain or loss of magnetic minerals) and the presence of volcanic glass. X_{total}: total magnetic susceptibility.

	MIS 5			MIS 3			MIS 1			
Profile	Corralito I	Corralito I	Lozada	Corralito I	Corralito II	Monte Ralo	Corralito I	Corralito II	Monte Ralo	Lozada
Layer	PaleosolIII	Paleosol II	Paleosol I	Paleosol I	Paleosol III	Paleosol I	Burried soil	Present soil	Burried soil	Present soil
X_{total}	↑		↓	↓	↑	↑	↑	↑	↑	↑
% Volcanic glass	20	60	95	20	40	70	30	40	25	40
Age [ka]	115 ka		105 ka	66.1 ±9.4 ka	43.4 ±3.3 ka	68.2 ±12.2 ka	311–474 cal. yrs BP 1945–2151 cal. yrs. BP			

weathering processes under relative more drier condition in comparison to the those of the other two outcrops (Corralito I and II). Surprisingly, the volcanic glass contents are very high, which could indicate poor devitrification due to climatic dry condition, or it could be caused by simultaneous deposition of volcanic material with the weathering processes. In either case, the magnetic signal of Monte Ralo profile could not be compared with the others outcrops cause the geological system was influenced by other climate, or volcanic additional input simultaneously with the pedogenesis. In the first case, another environmental condition, the hypothesis of contemporaneity proposed for the paleosols would not be strictly correct.

The analysis of the magnetic susceptibility (X_{total}) for the buried soil of Corralito I and Monte Ralo and the present soil of Corralito II and Lozada, which would correspond to MIS 1, show a gain in magnetic mineral. It is interpreted as pedogenic magnetic particles generation and preservation of the detrital magnetic minerals (Table 8). The gain of magnetic minerals would be controlled by a negative water balance, despite the abundant presence of volcanic glass in these soils (Table 8).

A notable fact is that soils and paleosols developed about in the same time interval have antagonistic magnetic responses, when it is assumed that the magnetic characteristics should be similar. These show that the magnetic properties are affected by many factors, such as the topographic position, paleosol development (which should affect permeability) and presence of volcanic glass.

Finally, the presence of smectite indicates devitrification during more intense or temporarily prolonged weathering. Consequently, the current content of volcanic glass might be related to the exposure time to pedogenic processes, and could not be precisely representative of the initial content in the parent material. This fact significantly complicates the quantitative interpretations of magnetic properties. At present, it is not possible to quantify certainly exposure time of paleosols to pedogenesis. Only qualitative interpretation can be done taking into account many variables of the geological system.

6. CONCLUSIONS

The sedimentary succession studied here is complex and cyclic and consists in loess deposit partially reworked with discrete sectors modified by pedogenesis. Paleosols have important development in the profiles and mark periods of no sedimentation and predominance of pedogenic processes; the evidence of bioturbation in many points of the analyzed section indicates that these processes were active as that sediment was deposited; also the pedogenic processes inferred decarbonatation-carbonatation, melanization and clay-illuviation are present in the analyzed profiles. The parent material of all profiles has a volcanic-pyroclastic origin, confirm by the presence of illite and smectite, clays which derive form the mineralogical alteration of this material. The magnetic signature between the profiles is modified by topographic position, paleosol development, volcanic glass content and mainly time of exposure to weathering and pedogenic processes. In this case, magnetic properties should not be a reliable proxy to analyzed paleoprecipitation. Only a multidisciplinary analysis can effectively explain qualitatively the climatic variations occurred in a particular environment with a particular substrate and geomorphological conditions inferred.

Acknowledgements: This work was funded by projects Agencia PICT 0382/07 and PIP 747/10. Geologist Pablo Eveling's collaboration in the fieldwork was vital to obtaining the present results and Gabriella Boretto for helping us in drawing the map. We also would like to thank to Petr Schnabl and an anonymous referee for their suggestions which help us to improve our paper.

References

Argüello G.L., Dohrmann R. and Mansilla L., 2012. *Loess of Córdoba (Argentine) Central Plain, present state of knowledge and new results of research.* In: Rossi A.E. and Miranda L.S. (Eds.), *Argentina: Educational, Geographical and Cultural Issues*. Nova Science Publishers, New York, 1–49.

Boyle J., Dearing J., Blundell A. and Hannam J., 2010. Testing competing hypotheses for soil magnetic susceptibility using a new chemical kinetic model. *Geology*, **38**, 1059–1062.

Capitanelli R., 1979. Geomorfología. In: Vázquez J., Miatello R. and Roqué M. (Eds), *Geografía Física de la Provincia de Córdoba.* Editorial Boldt, Buenos Aires, Argentina, 213–294 (in Spanish).

Evans M.E., 1999. Magnetoclimatology: a test of the wind-vigour model using the 1980 Mount St. Helens ash. *Earth Planet Sci. Lett*., **172**, 255–259.

Evans M.E, 2001. Magnetoclimatology of aeolian sediments. *Geophys J. Int*., **144**, 495–497.

Florindo F., Roberts A.P. and Palmer M.R., 2003. Magnetite dissolution in siliceous sediments. *Geochem. Geophys. Geosyst*., **4**, 1053, DOI: 10.1029/2003GC000516.

Forman S., Pierson J. and Lepper K., 2000. Luminiscense geochronology. In: Nollers J.S., Sowers J.M. and Lettis W.M. (Eds), *Quaternary Geochronology: Methods and Applications*. American Geophysical Union, Washington, D.C., 157–176.

Frechen M., Seifert B., Sanabria J.A. and Argüello G.L., 2009. Chronology of Late Pleistocene pampa loess from the Córdoba area in Argentina. *J. Quat. Sci. Rev*., **24**, 761–772.

Freytenet P., 1971. Paleosols résiduels et paleosol alluviax hydromorphes dan le Crétace superieur e l'Eocène basal en Languedoc. *Revue Géographie Physique et Geologie Dynamique*, **13**, 245–268 (in French).

Gale S.J and Hoare P.G., 1992. *Quaternary Sediments: Petrographic Methods for the Study of Unlithified Rocks.* Belhaven Press, London, U.K., 323 pp.

Gili E. and Gaiero D., 2014. South American dust signature in geological archives of the Southern Hemisphere. *Past Global Changes*, **22**, 78–79.

Imbellone P., 2011. Classification of paleosols. *Geociências*, **30**, 5–13.

Iriondo M., 1997. Models of deposition of loess and loessoids in the upper Quaternary of South America. *J. South Am. Earth Sci.*, **10**, 71–79.

Iriondo M. and Kröhling D., 1995. El Sistema Eólico Pampeano. Pampean eolic system. *Comunicación Museo Provincial de Ciencias Naturales Florentino Ameghino*, **5**, 1–68 (in Spanish).

Karlsson A., 1990. Aspectos del material piroclástico de los loess, Córdoba, Argentina. *Actas del XI Congreso Geológico Argentino*. San Juan, Argentina, 434–438 (in Spanish).

Kemp R.A., 2001. Pedogenic modification of loess: significance for palaeoclimatic reconstruction. *Earth Sci. Rev.*, **54**, 145–156.

Kemp R.A., Zárate M., Toms P., King M., Sanabria J.A. and Argüello G.L., 2006. Late Quaternary paleosols, stratigraphy and landscape evolution in the Northern Pampas, Argentina. *Quat. Res*., **66**, 119–132.

Kröhling D. and Carignano C., 2014. La estratigrafía de los depósitos sedimentarios cuaternarios. In: Matino R. and Guereschi A (Eds), *Relatorio del XIX Congreso Geológico Argentino*. Alsapema SA., Cordoba, Argentina, 673–724 (in Spanish).

Lisiecki L.E. and Raymo M.E., 2005. A Pliocene-Pleistocene stack of 57 globally distributed benthic δ18O records. *Paleoceanography*, **20**, PA1003, DOI: 10.1029/2004PA001071..

Maher B., 1998. Magnetic properties of modern soils and Quaternary loessic paleosols: paleoclimatic implications. *Paleogeogr. Paleoclimatol. Paleoecol.*, **137**, 25–54.

McCormac F.G., Hogg A.G., Blackwell P.G., Buck C.E., Higham T.F.G. and Reimer P.J., 2004. SHCal04 Southern Hemisphere Calibration 0 - 1000 cal BP. *Radiocarbon*, **46**, 1087–1092.

Muhs D.R. and Zárate M., 2001. Late Quaternary eolian records of the Americas and their paleoclimatic significance. In: Markgraf V. (Ed.), *Interhemispheric Climate Linkages*. Academic Press, New York, 183–211.

Munsell A.H., 1912. A pigment color system and notation. *Am. J. Psychol.*, **23**, 236–244.

Oches E.A. and Banerjee S.K., 1996. Rock-magnetic proxies of climate change from loess-paleosols sediments of the Czech Republic. *Stud. Geophys. Geod.*, **40**, 287–300.

Orgeira M.J. and Compagnucci R., 2006. Correlation between paleosol-soil magnetic signal and climate. *Earth Planets Space*, **58**, 1373–1380.

Orgeira M.J. and Compagnucci R.H., 2010. Uso de la señal magnética de suelos y paleosuelos como función climática.. *Rev. Asoc. Geol. Argentina*, **65**, 612–623 (inSpanish).

Orgeira M.J., Pereyra F.X., Vásquez C., Castañeda E. and Compagnucci R., 2008. Environmental magnetism in present soils, Buenos Aires province, Argentina. *J. South Am. Earth Sci*, **26**, 217–224.

Orgeira M.J., Egli R. and Compagnucci R., 2011. A quantitative model of magnetic enhancement in loessic soils. In: Petrovský E., Herrero-Bervera E., Harinarayana T. and Ivers D. (Eds), *The Earth's Magnetic Interior*. Springer-Verlag, Dordrecht, The Netherlands, 361–368.

Pasquini A.I., Lecomte K.L., Piovano E. and Depetris P.J., 2006. Recent rainfall and runoff variability in central Argentina. *Quat. Int*., **158**, 127–139.

Rouzaut S., 2015. *Estudio geológico y de magnetismo ambiental de secuencias sedimentarias asignadas al Cuaternario tardío, expuestos en la Llanura Pampeana, Córdoba (R. Argentina). Implicancias paleoclimáticas*.. PhD Thesis. Universidad Nacional de Córdoba, Córdoba, Argentina, 334 pp.

Rouzaut S., Orgeira M.J., Tófalo O.R., Vásquez C., Argüello G.L., Sanabria J. and Mansilla L., 2013. Estudio comparativo de propiedades magnéticas en la región central de la provincia de Córdoba, Argentina. *Geoacta*, **38**, 128–139 (in Spanish).

Rouzaut S.; Orgeira M.J., Vásquez, C., Argüello G.L. and Sanabria J., 2012. Magnetic properties in a loess-paleosol sequence of Córdoba, Argentina. *Rev. Soc. Geol. España*, **25**, 55–63.

Rouzaut S., Orgeira M.J., Vásquez C., Ayala R., Argüello G.L., Tauber A., Tófalo R., Mansilla L. and Sanabria J., 2015. Rock magnetism in two loess-paleosol sequences in Córdoba, Argentina. *Env. Earth Sci*., **73**, 6323–6339.

Siddall M., Chapell J. and Potter E.K., 2007. Eustatic sea level during past interglacial. In: Sirocko F., Claussen M., Sánchez Goñi M.F. and Litt T. (Eds), *The Climate of Past Interglacial*. Elsevier, London, U.K., 75–92.

Struiver M. and Reimer P.J., 1993. Extended ^{14}C database and revised CALIB radiocarbon calibration program. *Radiocarbon*, **35**, 215–230.

Teruggi M.E., 1957. The nature and origin of the Argentinean loess. *J. Sed. Petrol.*, **27**, 322–332.

Zárate M.A., 2003. Loess of southern South America. *Quat. Sci. Rev*., **22**, 1987–2006.